MINISTRY OF EDUCATION AND TRAINING

VIETNAM ACADEMY OF SCIENCE AND TECHNOLOGY

GRADUATE UNIVERSITY OF SCIENCE AND TECHNOLOGY

Nguyễn Văn Tiến

ENHANCEMENT FEATURES OF SERS SUBSTRATE MFON STRUCTURE AND DEVELOPMENT OF PORTABLE RAMAN DEVICE

Specialized: Solid-state physics
Code: 9 44 01 04

SUMMARY OF THE DOCTORAL THESIS

Hà Nội - 2023

This work was completed at: *Graduate University of Science and Technology - Vietnam Academy of Science and Technology.*

Science supervior:

1. TS. Nguyễn Minh Huệ

2. PGS. TS. Nghiêm Thị Hà Liên

Reviewer 1: …
Reviewer 2: …
Reviewer 3: ….

The thesis will be defended before the Academy level doctoral thesis evaluation committee, meeting at *Graduate University of Science and Technology - Vietnam Academy of Science and Technology in ... hour ..', date ... month ...year 202.*

The thesis can be found at:

- Library Graduate University of Science and Technology

- National Library of Vietnam

INTRODUCTION

1. The urgency of the thesis

The Raman spectroscopy method was developed to study molecular vibrations, thereby discovering the molecule's structure, symmetry, electronic structure, kinetics, and chemical bonding. Due to technological barriers such as high-intensity monochromatic light source, high-resolution spectrometer, low noise background, sensitive optical receiver, etc., until the late 1980s, Raman spectroscopy has become a popular method in the study of chemical compounds qualitatively as well as quantitatively.

The advent of Fourier transform Raman (FT-Raman) Raman spectroscopy, CCD optical receivers, laser sources, and interference filters has revolutionized Raman spectroscopy, further expanding the fields of application areas of this method.

Recently, the appearance of portable/handheld Raman spectrometers on the market has been creating the third wave in the development history of the field of Raman spectroscopy. The idea behind this generation of devices is not only to create a compact spectrometer that can be brought to the field and perform spectroscopy but also to create a device that helps users and non-specialists quickly get answers for their business. The question may be whether the quality of the input materials is guaranteed? is the substance to be detected in the sample? what chemical is this sample, and what is the main ingredient? Can this liquid be brought on board?.... The computing power and speed of modern microprocessor chip generations, cloud computing technology, along with quantification algorithms, machine learning, and artificial intelligence AI enables this idea to be realized on a compact device.

The Raman spectroscopy method possesses the strength of being able to quickly give characteristic information, such as fingerprints of chemical substances, and can be applied to many different types of materials in solid, liquid, and gas. In addition, Raman spectroscopy is a non-contact, non-destructive measurement method that requires no sample preparation – usually just point-and-shoot. In particular, some Raman spectrometers have an optical system configuration that allows measurement of packaging, through protective layers of samples such as plastic and glass. These preeminent and user-friendly properties make Raman spectroscopy equipment increasingly popular in activities of security forces, border guards, environmental incident handling, chemical prevention, etc. The compact size and universality of portable/handheld Raman devices also allow their integration into the production lines of industries such as chemicals, biology, pharmaceuticals, and oil and gas. In particular, in the context of the development of 4.0 technology, the Internet of things (IoT) technology platform, portable Raman devices have a lot of potential in the field of sensor manufacturing for production line monitoring technology PAT (processes analytical technology).

Besides the strengths, Raman spectroscopy also has limitations. A major weakness is the low intensity of Raman scattering signals, so this method is difficult to apply to cases where it is necessary to identify and analyze trace samples with low concentrations. Many Raman spectroscopy techniques have been developed to overcome this weakness such as forced Raman spectroscopy, anti-Stoke coherent Raman spectroscopy (CARS), enhanced Raman scattering based on the TERS metal spike effect, and enhanced Raman scattering of the SERS surface. Among the above-mentioned methods, the SERS method does not require much equipment such as an ultra-short

pulse laser, nanometer shifter for the tip, etc., and can be used in combination with conventional Raman spectrometers. The SERS substrates can help to enhance the Raman signal by a factor of 10^8 or even higher, allowing spectroscopic measurements of single molecules. Since its accidental discovery in the early 1970s, a great deal of research has been carried out to understand the physical nature and explain the mechanism of surface Raman signal enhancement, different fabrication methods and applications. Application studies combining SERS substrates with portable Raman spectrometers have also been published in recent years. This includes research in difficult and demanding health and food safety fields.

With the increasing demand for SERS substrates, commercial SERS substrates have appeared on the market, supplied by more than ten manufacturers, including major brands such as Horiba, Ocean Optics, Silmeco.... At present, the cost of commercial SERS substrates is still high, and not commensurate to be used as consumables. Much research is still being done, on the one hand, to increase the performance of the SERS substrate, on the other hand, to find methods and materials to make the SERS substrates at low cost, or can be reused.

The topic of SERS has also been studied by a research group from the Institute of Materials Science, Vietnam Academy of Science and Technology, and has achieved many achievements. The team has developed a method to fabricate SERS substrates based on silver nanoparticles on silicon substrates and silver nanoparticles attached to silicon nanowires to detect organic matter at low concentrations. In particular, the group has developed the SERS method to solve the painful problem in Vietnam which is to detect traces of pesticides and plant protection substances.

Besides these large groups, the Raman spectroscopy method is interested in research, development, and application in many other units such as the Institute of Physics, Hanoi National University of Education, Thai Nguyen University, and Vietnam Japan University. , Institute of propellants - explosives... However, according to our research, when this thesis began to be researched, the construction of a portable Raman measuring system in general and a Raman device serving security surveillance in particular is still open in Vietnam. Moreover, the research on SERS substrates is still in favor of finding manufacturing methods without going into understanding the physical phenomena and processes to be able to optimize them.

2. Research objectives of the thesis

Within the framework of this thesis, three major goals have been set:

- One is to build and test a portable Raman spectrometer that is application-oriented for security inspection.

- The second is to study and fabricate a substrate to enhance SERS surface Raman scattering based on structures with large periodicity. Structures of this kind allow, on the one hand, to compare experimental results with theoretical simulations. On the other hand, the periodicity property enables the SERS substrates of this type to have the obtained Raman spectra achieving spatial uniformity when collecting signals from different positions of the substrate and high repeatability. These factors are extremely important, helping to optimize the performance of the fabricated SERS substrates. Specifically, the research focuses on improving the performance of the SERS substrate by reducing the scattering channel into the waveguide modes of the substrate.

- Compared to standard Raman spectrometers in the laboratory, portable machines usually have a lower sensitivity so the laser usually has a higher power to compensate for the signal quality. However, the large laser power can easily lead to burning, destroying the sample or the SERS substrate. Therefore, the third goal is to develop a method of measuring samples on the SERS substrate to avoid the above limitations so that the use of the SERS base can be combined with a portable spectrometer.

3. The main research contents of the thesis

To achieve the set objectives, the following research contents were carried out by the Ph.D. student:

a) About building experimental systems, developing and testing equipment

- Design and manufacture of portable Raman spectrometer using 638 nm diode laser and Avantes mini spectrometer. Survey to evaluate the sensitivity and resolution of the manufactured equipment.

- Studying raw spectral processing algorithms including noise filtering and fluorescent background types.

- Using equipment to collect and build Raman spectral libraries of some common explosives. Research algorithm to automatically identify explosives by comparing the obtained spectrum with the standard spectrum library.

- Design, and manufacture a random sample table, and test and compare the method of collecting random sample scanning spectrum with the traditional method of projecting and collecting spectra at a point.

b) Fabrication and optimization of SERS substrates based on metal film structure on polystyrene microspheres (MFON):

- Research to fabricate polystyrene microspheres with high uniformity and controllable size in the range of 200 nm to 1000 nm.

- Fabrication of close-packed monolayer polystyrene bead films and highly cyclic structures.

- Research on the fabrication of SERS substrates based on metal film structure on polystyrene microspheres. Building a theoretical model and simulation of surface Raman scattering due to near-field focusing effect, thereby optimizing the performance of the fabricated SERS substrate.

CHAPTER 1. OVERVIEW

The Raman spectroscopy method has transformed from a method that requires high-tech equipment, technically qualified operators, and basic training, to a method that is integrated into equipment. Compact portable/hand-held device that an ordinary technician can also use for his or her job. After more than 90 years since the phenomenon of Raman scattering was discovered, there are countless research papers, textbooks, and reference books that present the physical nature of Raman scattering, and the application of Raman spectroscopy in research structure and kinetics of molecules, and many other fields. Within the framework of the thesis, this chapter focuses on presenting an overview and synthesizing information about recent achievements in the field of portable Raman spectroscopy devices, to enhance surface Raman scattering and potential applications benefits of combining handheld Raman devices with SERS bases.

CHAPTER 2. SYNTHESIS OF POLYSTYRENE PARTICLES AND FABRICATION OF CLOSE-PACKED MONOLAYER OF THE POLYSTYRENE MICROSPHERES

This chapter of the thesis presents the research results of manufacturing polystyrene (PS) microspheres with high uniformity and variable size, controllable in the range of 200 to 1000 nm. Studies using these PS microspheres to fabricate close-packed monolayer of the PS microspheres for the fabrication of SERS substrates are also mentioned. This is one of the main goals of this thesis. Before going into details on the fabrication of PS microspheres and monolayer films, the methods of making SERS substrates based on microspheres are also reviewed and presented below.

2.1. Synthesis of polystyrene microspheres

In this thesis, the emulsion polymerization method is used to fabricate PS microspheres. This method is simple to implement, requiring only a few basic tools to produce high-quality, controllable single-dispersion microspheres.

PS microspheres are produced during emulsion polymerization of styrene in solutions of sodium lauryl sulfate (SDS), potassium persulfate (KPS), and ethanol as emulsifier, reaction initiator, and diffusion medium respectively.

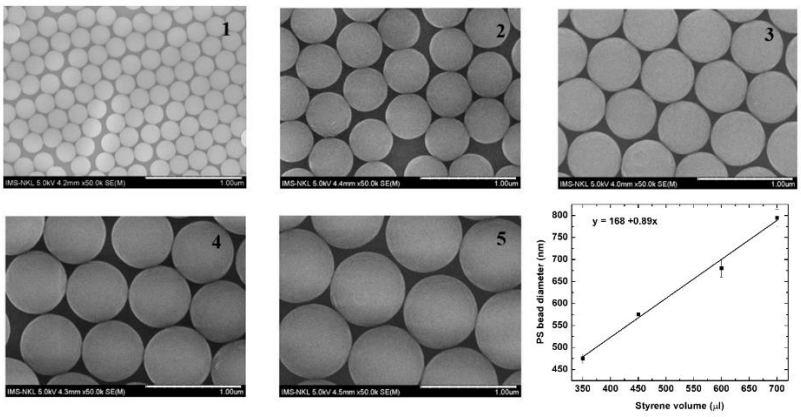

Figure 2.3. The image of the prepared PS particles and the graph of the size of the PS particles depending on the volume of styrene added to the reaction.

The size of PS particles is controlled by the amount of styrene added to the reaction. To obtain high-quality, monodisperse, nearly spherical, and highly uniform PS particles, the amount of potassium persulfate and sodium lauryl sulfate in each 70 ml of ethanol alcohol solution was determined by the following formula:

$$W = W_0(V / 4.5)$$

where W and W_0 are the mass, in grams, of potassium persulfate and sodium lauryl sulfate, respectively, and V is the volume of styrene (measured in milliliters) added to the reaction.

PS particles with sizes between 200 and 1000 nm can be easily synthesized by this method. The quality of the PS particles can be easily seen in the SEM images (Figure 2.3). The standard deviation of the diameters of the synthesized particles is less than 5%. The particle size is linearly dependent on the amount of styrene added to

the reaction (graph in Figure 2.3). This property can be used to change the optimal PS particle size for each application, such as optimizing the SERS substrate for different excitation laser wavelengths.

2.2. Fabrication of close-packed monolayer of the polystyrene microspheres

2.2.1. Formation of close-packed monolayer of the polystyrene microspheres

The close-packed monolayer of the polystyrene microspheres has many roles and applications as outlined above. Many methods of making these films have been researched and developed, such as spin coating, Langmuir-Blodgett method, and drop-rescue method. Which, the drop-rescue method is relatively simple, does not require special tools, and creates a large sample area as illustrated in Figure 2.4.

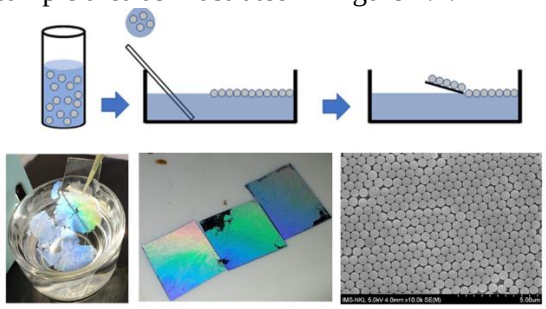

Figure 2.4. Schematic diagram of the fabrication process of close-packed monolayer of the polystyrene microspheres.

2.2.2. Creating cyclic structures using microspheres by oxygen plasma etching technique

In this study, the distance between PS particles on a close-packed monolayer film was adjusted in a low-pressure oxygen plasma. The optimized process parameters are 0.5 mbar pressure, 240W RF power, and 200 sccm oxygen flow rate. Under this condition, the diameter of the particles is slightly reduced by uniform etching over the entire surface area of the grain while retaining the spherical shape. Figure 2.6 a)-c) is the SEM image of the monolayer film close-packed with PS particles after 0, 4, and 40 min of etching in oxygen plasma, respectively. During the first ten minutes, the corrosion rate is almost linear reaching about 14 nm per minute. The particles reduced their initial diameter from 574 nm to 510 nm after being etched for 4 min; to 410 nm after 12 min. This corrosion rate is moderate, allowing precise control of the gap width. However, as the corrosion time was further increased, the corrosion rate became exponentially slower (Figure 2.6d). This could be due to the accumulation of charge on the PS particles. A potential barrier prevents oxygen ions from interacting with the PS particles, thereby slowing the rate of corrosion. As shown in Figure 2.6d, the experimental data points fit an inverse exponential function.

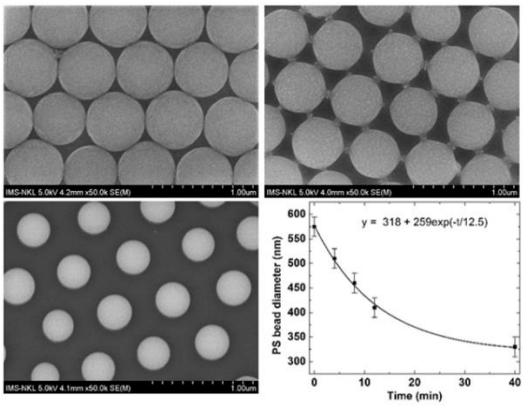

Figure 2.6. a)-c) SEM image of the monolayer film close-packed with PS microspheres with a diameter 574 nm after 0, 4, and 40 min of etching in oxygen plasma, respectively; d) Graph of the change of PS particle diameter over time of corrosion.

2.3. Developing a method to determine PS particle size by transmission spectroscopy

2.3.1. Transmission spectrum of a monolayer film of packed polystyrene microspheres

The transmission spectroscopy results for PS 574 nm microspheres are shown in Figure 2.7. While the dashed lines are smooth and have no special position, the spectral line of close-packed monolayer films appears minimal. This minimum position shifts towards the long wavelength as the size of the PS microsphere increases (Figure 2.8). Theoretical works show that for a monolayer film close-packed with ideal PS microspheres ($\varepsilon_{sphere} = 2,56$), the positions of the minima in the transmission spectrum appear at a wavelength such that the parameter $Z = \left(\sqrt{3}d\right) / 2\lambda$ satisfies the conditions $Z = 0.71, 0.85, 1.00, 1.34, 1.55$.

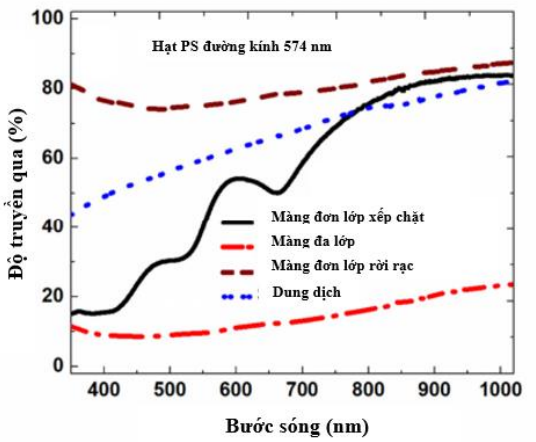

Figure 2.7. Transmittance spectra of unpacked monolayer film (brown line); PS granule solution (blue line); close-packed monolayer film (black line); disordered granular multilayer membrane.

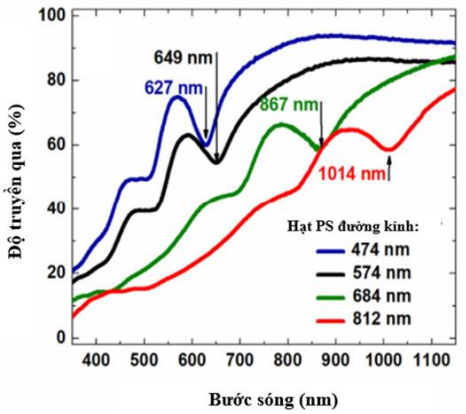

Figure 2.8. Transmittance spectrum of the monolayer close-packed PS microsphere particles: PS 477 nm-blue; PS 574 nm-black; PS 684 nm-green; PS 812 nm-red.

2.3.2. Simulation model of close-packed monolayer polystyrene film

For the calculation, we use the FDTD method in the CST simulation software to simulate the transmission spectrum of the monolayer close-packed with the PS microspheres. The structure of the model is simulated as a monolayer film close-packed with dielectric particles with a dielectric constant ε_{sphere} on a dielectric substrate with dielectric constant ε_{sub}. As shown in Figure 2.9a the first layer of the base unit cell consists of a sphere with diameters in contact with the quadrants of the sphere at the corners, the second layer of the unit cell is a dielectric substrate with a thickness of t_d.

The incident electromagnetic wave is perpendicular to the surface of the structure. The electric and magnetic field components of the electromagnetic wave are directed along the Oy and Ox axes, respectively. The emitter and receiver are placed on either side of the structure along the Oz axis to measure the transmitted scattering parameters of the electromagnetic waves when interacting with the PS microspheres monolayer film and the dielectric substrate. Then the transmittance (T) is determined by the expression:

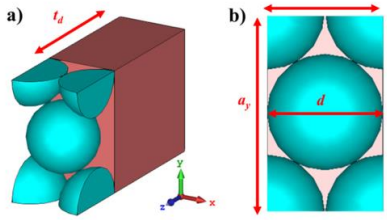

Figure 2.9. The base unit cell for calculation of monolayer film close-packed with microspheres PS on dielectric substrate: a) perspective view; b) top-down view.

2.3.3. Simulation results of the transmission spectrum of a close-packed monolayer polystyrene film

Figure 2.10 shows the calculation results of the transmission spectrum when the dielectric constant of the substrate varies between 1.5 and 3. This range of dielectric constants covers all typical glass substrates today. When the dielectric constant of the substrate changes between 1.5 and 3, the position of the first minimum ($Z = 0.7$) is almost unchanged while the position of the second minimum ($Z = 0.85$) is blue-shifted (15 nm).

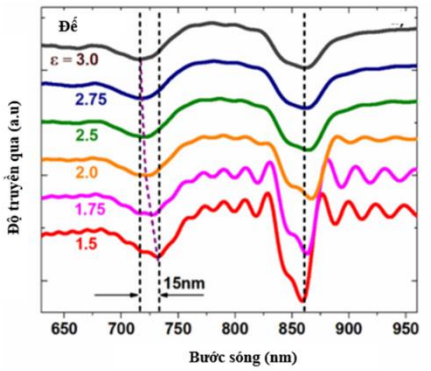

Figure 2.10. The results of calculating the transmittance spectra of a monolayer film close-packed with PS microspheres with a diameter 701 nm on a dielectric substrate with the dielectric constant of the PS microspheres $\varepsilon_{sphere} = 2.25$ and the dielectric constant of the substrate varying from 1.5 to 3.

The simulation results of the transmission spectrum of the monolayer film close-packed with PS microspheres on the glass substrate are compared with the experimental results and shown in Figure 2.12. Simulation lines all appear at the minimum position at the wavelength position that coincides with the minimum position of the experimental lines. Since the experimental PS microspheres are not ideal 2D photonic crystals, the coverage is lower than that of the ideal particle films used in the calculations, resulting in the experimental transmittance being larger than the simulated transmittance. In addition, because of the imperfections of the experimental PS microsphere monolayer films, the minima almost disappeared on the transmission spectrum. Only the first minimum ($Z = 0.7$) is still discernible on the transmission spectrum.

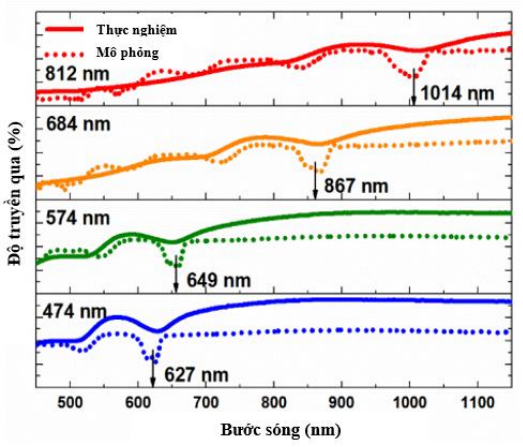

Figure 2.12. Transmission spectrum of monolayer film close-packed with microspheres PS: solid lines are experimental results and dashed lines are simulation results. Simulation parameters are $\varepsilon_{sphere} = 2.25(\mathrm{n} = 1.5)$ and $\varepsilon_{sphere} = 2.25(\mathrm{n} = 1.5)$, the diameters of the PS microspheres are: 507, 525, 701, and 820 nm.

2.3.4. Experimental results

The relationship between the PS microsphere diameter and the minimum position wavelength on the transmission spectrum of the monolayer film close-packed with the PS microspheres is shown in Figure 2.13. These data points are fitted using a simple linear function with a slope of 0.799. The parameter calculated by the

slope of the graph is $Z = 0.69$, this value is consistent with the theoretical value $Z = 0.7$. This result confirms the correctness of the theoretical model.

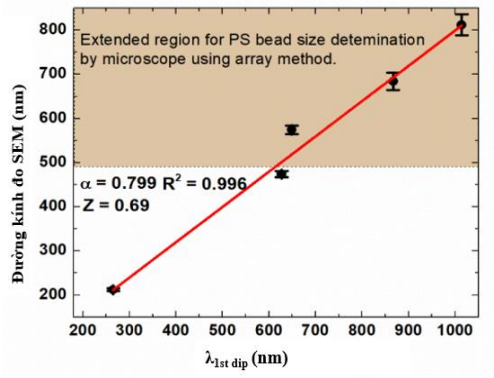

Figure 2.13. Graph showing the diameter of the PS microsphere against the wavelength of the position of the minimum in the transmission spectrum. The parameter determined by the slope of the graph is equal to $Z = 0.69$, which is consistent with the theoretical value used in the simulation.

CHAPTER 3. OPTIMIZE PERFORMANCE MFON STRUCTURE SERS

This chapter presents the results of the graduate student's research on the fabrication, optimization, and performance improvement of the SERS substrate with MFON structure by suppressing the signal loss channel into the substrate.

3.1. Optical properties of the MFON structure

3.1.1 SERS surface Raman scattering enhancement effect on MFON structure

Greeneltch and colleagues demonstrated the ability to scale up the fabrication of MFON-structured SERS substrates, investigated and evaluated the features of enhanced surface Raman scattering over a large area. As shown in Figure 3.1, the MFON structure can be fabricated on an area as large as that of a commercial 10 cm diameter silicon wafer. The Raman scattering enhancement factor EF was experimentally investigated at 9 different positions on the plate. At each site, the Raman scattering signal of ethanolic benzenethiol was measured in five rows from A to E, each row of 10 measurement points. The mean value of the enhancement factor EF and standard deviation are shown in Figure 3.1d. On the whole slab enhancement factor $EF = 4.23(\pm 8.6\%) \times 10^7$.

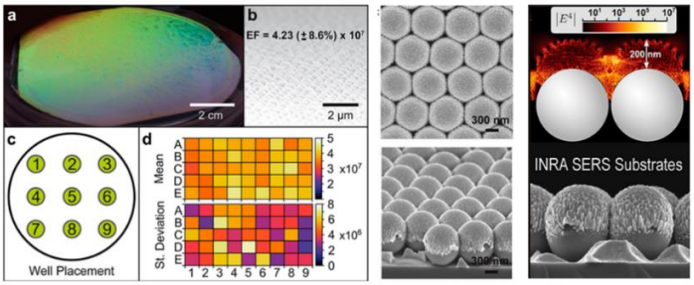

Figure 3.1. Fabrication of the MFON structure SERS substrate with high uniformity on the silicon wafer, near-field distribution, and hot spots.

The diffuse reflectance spectrum of the MFON structure has a minimum region corresponding to the LSPR surface plasmon resonance. The LSPR resonance wavelength of this structure depends on the size of the microspheres used. By changing the size of the microsphere, we can tune the resonance wavelength in a fairly wide range from 330 nm (160 nm microsphere) to 1838 nm (1490 nm microsphere) as shown in Figure 3.2b.

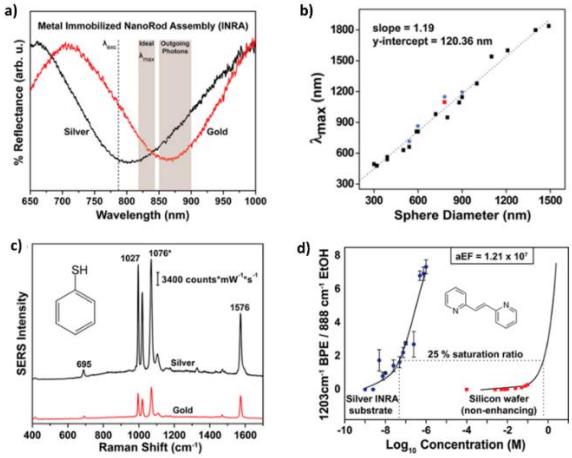

Figure 3.2. Optimized MFON structure SERS substrate for different excitation laser wavelengths.

3.1.2. Anomalous transmission spectrum of the MFON structure

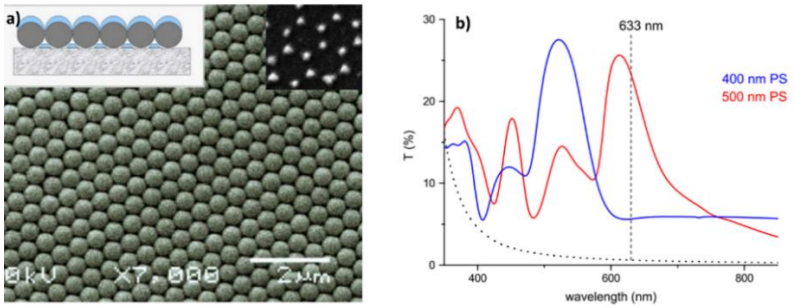

Figure 3.4. SEM image and model of MFON structure, the anomalous transmission spectrum of MFON structure.

The anomalous transmission spectrum of the MFON structure was detected by Farcau et al. Figure 3.4b is the transmittance spectrum of the silver-coated MFON structure on the 400 and 500 nm PS particles (blue and red lines in Figure 3.4b, respectively). Compared with the transmittance spectrum of the silver layer of the same thickness (dashed line), there are distinct transmittance peaks. The position of the transmission spectral peak depends on the size of the PS particle. The phenomenon of light transmission anomaly of the MFON structure is similar to the phenomenon of light passing through an array of holes smaller than the wavelength on the metal plate - EOT.

3.2. Fabrication and characterization of the MFON structure SERS substrate

3.2.1. Fabrication of the MFON structure SERS substrate

Close-packed monolayer films from 212±3, 477±7, 574±10, 684±20, and 812±24 nm polystyrene particles after being trapped and compacted on the water surface (as described in Chapter 2), are picked up on a clean silica pad and a silver coated silicon pad. After being allowed to dry naturally, a layer of silver with a thickness of 200 nm was coated on them by electron beam evaporation. This thickness of the silver layer is selected by the optimal research results of Zao Yi and colleagues, furthermore to ensure that the background spectrum of the PS microsphere layer is completely blocked. The silver layer was removed using a Leybold Univex 400 electron beam evaporator, at a vacuum of 5×10^{-6} Torr and a flight speed of 5 Å/s. The thickness of the metal film is controlled through a quartz sensor.

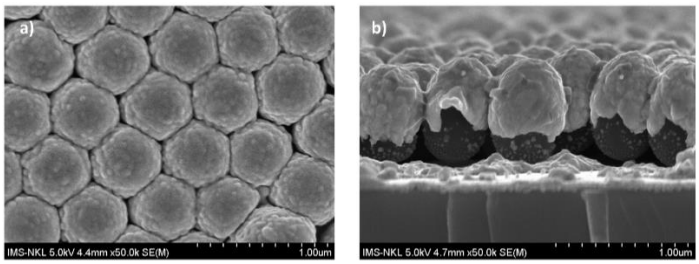

Figure 3.5. Cross-sectional SEM image of the MFON structured SERS substrate on the metal substrate.

3.2.2 Investigation of optical properties and ability to enhance Raman scattering of MFON structured SERS substrates

To study the optical properties of the fabricated MFON-structured SERS substrates, we measured the reflectance spectrum of the MFON-structured SERS substrates with different PS particle sizes on silicon. Unlike the reflectance spectrum of the silver film on the flat substrate, the reflectance spectrum of the MFON structure substrate on silicon appears wide hollows. The position wavelength of the cavity is determined by the size of the PS particle and can be adjusted from visible to infrared. These depressions are associated with surface plasmon resonances that depend on the size of the PS particle.

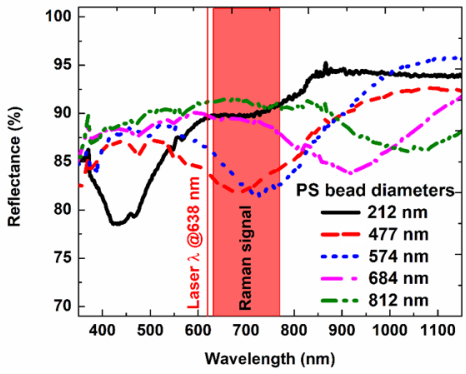

Figure 3.6. The reflectance spectrum of MFON-structured SERS substrates on silicon.

Figure 3.7 presents the recorded reflectance spectrum of MFON on the metal substrate and the silicon substrate. These two reflectance spectra are almost similar, except that the reflectance spectrum of the structure on

the metal layer is higher than that of the MFON structure substrate on silicon, and the recess wavelength has a shift to the violet region.

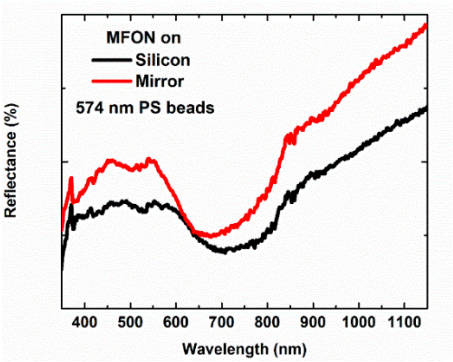

Figure 3.7. Reflectance spectra of the MONG structure SERS substrate in silicon and on the metal layer.

Figure 3.8 and Figure 3.9 show the results of Raman spectroscopy of 10^{-6} M Rhodamine 6G solution using MFON-structured SERS substrates on silicon and the base metal layer. The intensity of the Raman peaks of Rhodamine 6G increased and peaked when the PS particle diameter increased from 212 to 477 nm. Continuing to increase the PS particle size, the intensity of the Raman peaks of Rhodamine 6G decreased. This changing trend can be understood from the electromagnetic mechanism of the SERS effect. According to the electromagnetic mechanism, the enhancement effect will be strongest when the localized surface plasmon resonance wavelength is in the region between the wavelength of the laser source and the wavelength of the Raman scattered photon. As shown in Figure 3.6 the wavelength of the excitation laser source is 638 nm marked with the red vertical line and the wavelengths of the Raman Stokes scattering and marked as the corresponding red rectangular band. The wavelength at the concave position on the reflectance spectrum of the MFON-structured SERS substrate shifts towards the long wave from the blue region to the infrared region when the particle diameter changes from 212 to 812 nm. For the SERS substrate, the MFON structure is fabricated based on the PS particle with a diametof er 477 nm, the localized surface plasmon resonance wavelength, and the scattering wavelength satisfy the above-analyzed maximum enhancement condition. Therefore, the SERS substrate based on the 477 nm diameter PS particle achieved the strongest enhancement performance. This result is consistent with those reported by Greeneltch and Yi.

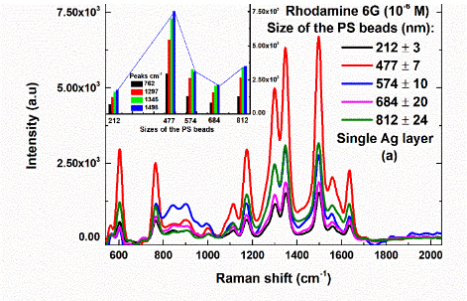

Figure 3.8. Results of measuring SERS of Rhodamine at a concentration of 10-6 M using MFON structure substrates on silicon.

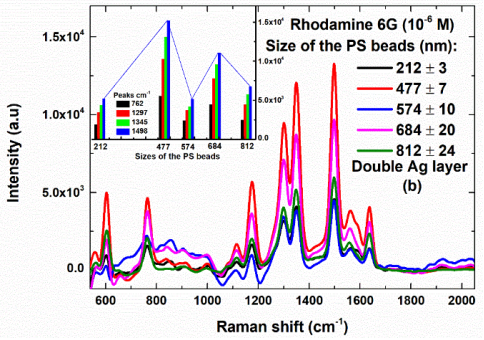

Figure 3.9. Results of measuring the SERS of Rhodamine at a concentration of 10^{-6} M using the MFON structure substrate on the base metal layer.

Figure 3.10 shows the Raman spectrum of Rhodamine 6G on MFON-structured SERS substrates fabricated from PS 477 nm particles on silicon and the base metal layer. The effect of the metal backing on the performance of the MFON-structured SERS substrate can be seen. The intensity of Raman peaks in the region from 500 to 1800 cm-1 is doubled. This effect is also observed for SERS substrates fabricated from PS particles of different sizes as shown in the inner figure of Figure 3.9. Thus, the base metal layer improves the Raman signal enhancement performance by several times in the PS particle size range from 200 to 800 nm.

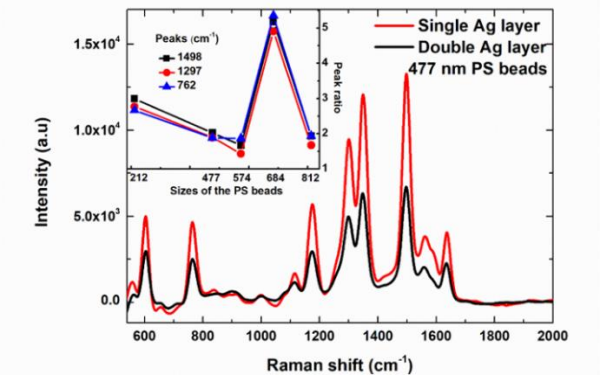

Figure 3.10. Raman spectrum of 10^{-6} M Rhodamine 6G on MFON structured SERS substrate with PS particle diameter of 477 nm: black line on a silicon substrate; Red line base on the base metal layer. The upper left inset is the ratio of the Raman peak intensity of R6G on different MFON structure substrates.

3.3. Simulation of optical properties of the MFON structure

To study the influence of the base metal layer on the MFON structure, we simulated the reflection spectrum and electric field distribution in the MFON structure on silicon and on the base metal layer by 3D FTDT using the software. CST trade simulation. The simulated reflectance spectrum is further processed by a fast Fourier transform (FFT) filter to remove the high-frequency components.

The simulation results of the reflection spectrum of the MFON structure are presented in Figure 3.12: the black dashed line is the reflectance spectrum of the MFON structure on silicon and the red solid line is the reflectance spectrum of the MFON structure on the metal layer. background type. The simulated spectrum that qualitatively repeats the experimental results is shown in Figure 3.7. The bottom silver layer is separated from the silver tip by a monolayer membrane close-packed with 500 nm PS particles. However, it can still affect and significantly increase the reflectivity of the MFON structure in the resonance region.

When studying the reflectance spectrum of the MFON structure on the silicon substrate and the metal layer, it is observed that the metal layer makes the reflectivity significantly higher in the hollow region, the longer wavelength is more affected Figure 3.12. This wavelength asymmetric effect of the active metal mirror layer is beneficial for backscatter SERS measurements.

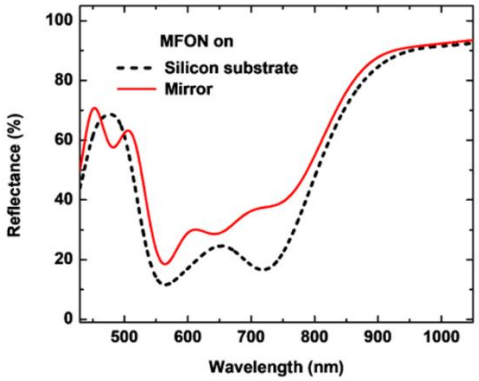

Figure 3.12. Simulation results by software CST reflectance spectrum of MFON structure on silicon and metal layer. The parameters used for simulation are as follows: the diameter of the PS beads $d = 500\,nm$, the silver film thickness, and the thickness of the substrate $t_d = 500\,nm$. The dielectric constants of the PS (ε_p) and silicon (ε_s) spheres varying with light frequency in the optical region are directly extracted from the published experimental results.

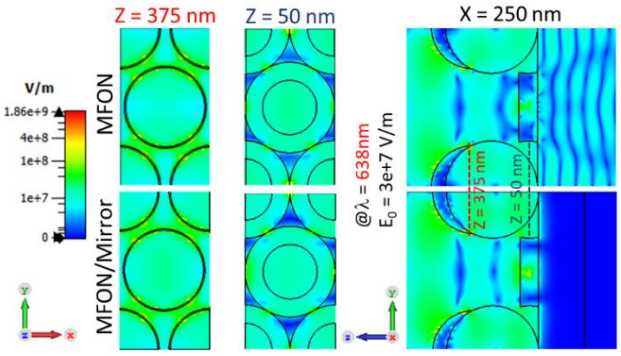

Figure 3.13. Simulation results of electric field distribution on the MFON structure on silicon and the base metal layer. The base metal layer changes the local field distribution of the MFON structure. It prevents the field from penetrating the substrate.

Figure 3.13 shows the electric field distribution simulated by CST in the MFON structure on silicon and in the MFON structure on the metal layer. The top-down images show hot spots where a highly concentrated

electric field is located at the junction between the microspheres. The electric field increased nearly 100 times for the MFON structure on the silicon substrate. Converting to the SERS enhancement factor ($EF = (E/E_0)^4$), we get an EF of size 10^8. Besides, the base metal layer changes the local field distribution on the MFON structure on the base metal layer.

The side view shows more locations of hotspots. They occur at the rim of the silver caps, at the base of the sphere, between the microspheres, and the silver triangle. The metal coating does not change the pattern of the field. It helps to further focus the electric field at hot spots. In addition, the mirror metal layer prevents the field from leaking into the substrate, which explains the increased reflectivity of the MFON structure on the metal layer.

CHAPTER 4. BUILDING PORTABLE RAMAN SPECIFICATION EQUIPMENT

This chapter presents the research results and solutions that have been applied in building a portable Raman spectrometer during the Ph.D. student's thesis. In particular, the content focuses on detailing the design and structure of the device and techniques to improve signal quality such as noise filtering algorithm, fluorescence background removal, automatic spectrum recognition algorithm, etc. dynamic, random sampling technique.

4.2. Building a portable Raman spectrometer system

4.2.1. Portable Raman spectrometer using 638 nm laser

A frequency-stabilized diode laser using a mass hologram grating (VHG) from Ondax was used as a monochromatic light source that excites the Raman scattering spectrum. The size of the laser is relatively compact (25.4 mm × 76.2 mm), which is relatively easy to integrate into portable devices. The emission wavelength of the laser was stabilized at 638 nm, with a spectral width of 0.05 nm.

Figure 4.3b) shows the sensitivity curve of the Avantes mini spectrometer that will be integrated into a Raman spectrometer. The excitation light wavelength of 638 nm was chosen to reduce the fluorescence background, and still ensure that the Raman scattering signal was in the maximum spectral sensitivity region of the spectrometer.

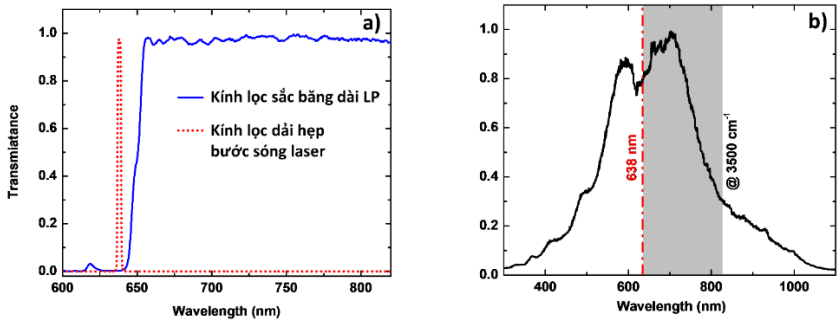

Figure 4.3. a) Transmission spectra of the narrow band and long band LP filter noise filter b) Sensitivity spectrum of the mini spectrometer.

From the above parameters of the selected optical components, it can be seen that the built Raman spectrometer will ensure effective measurement in the measuring range from 290 cm^{-1} to 3500 cm^{-1}. This is also

the common range of portable Raman spectrometers and also ensures enough characteristic information to be able to identify the material. Figure 4.4 is a snapshot of the built-in portable Raman spectrometer.

Figure 4.4. Photograph of the structure of a portable Raman spectrometer using a 638 nm laser.

4.2.2 Survey and evaluate the operation of the experimental portable Raman spectrometer

The device was tested by measuring the Raman scattering spectrum of ethanol alcohol at different concentrations. Figure 4.7 is the Raman spectrum of alcohol at concentrations from 10% to 100%. The results obtained are quite similar to other publications, but the spectral resolution is still poor. The device has not completely resolved the two lines 1055 cm^{-1} and 1090 cm^{-1} when viewed with the eye. When analyzing the band spectrum 1000 cm-1 can be seen that this spectral band is the superposition of two spectral lines at the position 1050 cm^{-1} and 1090 cm^{-1}. The instrument's 40 cm^{-1} spectral resolution is matched and dictated by the low resolution of the 1.2 nm mini spectrometer (corresponding to 19 cm^{-1} at 900 nm) used.

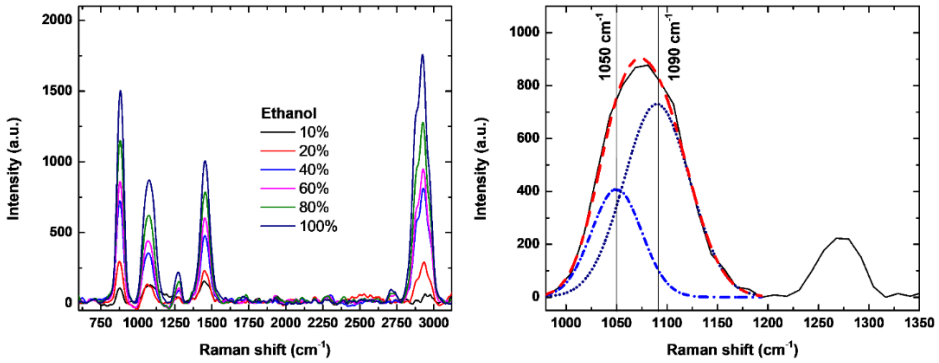

Figure 4.7. Raman spectra of ethanol at different concentrations.

The device's sensitivity threshold to RDX explosives was also tested. High-purity RDX explosive powder was diluted in acetone and determined to the smallest concentration that still determined the characteristic Raman spectrum of RDX. Figure 4.9a shows the Raman scattering spectrum of acetone and acetone with the addition of RDX (40 mg/ml). At a glance, the two spectrums are almost the same, but when zooming in to the range of 900 - 1400 cm^{-1}, there are still small differences. After normalizing the band signal in the region of 3000 cm^{-1} and subtracting the two spectrums, we obtain a solid line blue spectral line as shown in Figure 4.9b. This spectral line completely coincides with the Raman spectrum of the RDX crystal (dashed red line). The spectrum clearly shows the characteristic spectral peaks at positions: 1350 cm^{-1} (symmetric vibration mode of NO_2 group); 1590 cm^{-1} (asymmetric oscillation of NO_2 group); 1200 cm^{-1}, 1400 cm^{-1} (folding mode of group C −H); 860 cm^{-1}, (oscillation mode of group C −N −C); 890 cm^{-1} (loop breathing oscillation mode) is consistent with the structure of the RDX molecule and other publications. In this figure, we also see that, at the wave number region of 900 cm^{-1}, the two

spectral peaks of 890 cm^{-1} and 860 cm^{-1} are almost overlapping because the resolution of the device is not high, as shown in Fig. above.

At a concentration of 40 mg/ml, the strong scattering peaks were still clear, but the weaker peaks were mixed in the noise. Therefore, this RDX concentration is considered to be the minimum threshold that can be determined.

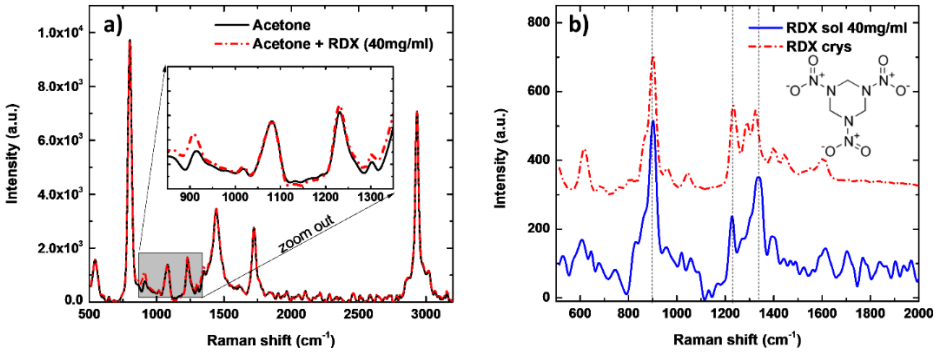

Figure 4.9. Raman spectrum of RDX explosive: Dotted line– Raman spectrum of pure RDX; Solid line – Raman spectrum of RDX in acetone (40mg/ml).

4.2.3 Spectral smoothing algorithm and fluorescence background noise type

Raw Raman spectra were smoothed by the Savitski–Golay method. The Savitski - Golay method has outstanding advantages in its ability to eliminate noise without shifting the position of the spectral peaks and not distorting (expanding) the peaks of the spectrum.

To fully automate the subtraction of the fluorescent background, in the software, the adaptive polynomial function matching method was used. After each polynomial match with the baseline, the software will automatically compare, if the value of the spectral line is greater than the polynomial line, it will be assigned equal to the value of the polynomial line. Then the function matching is performed again with the corrected spectral curve. In this way, the influence of the spectral peak on the polynomial fit line will be reduced gradually after each interaction step.

4.2.4 Spectral identification algorithm

Due to the characteristic of Raman scattering spectra of different substances. By comparing and contrasting the Raman spectrum obtained with the spectrum in the sample spectrum library, we can identify the substance being measured. This comparison can be done automatically through spectral similarity evaluation functions.

The correlation coefficient is a measure of the similarity between two signals. The correlation coefficient has a value in the range [0,1], the larger the correlation coefficient, the higher the similarity. When compared with the spectrum library, if the correlation coefficient is greater than the preset threshold value, the name of that

spectrum will be assigned in the library. The threshold value of the correlation coefficient is determined experimentally.

4.3. Random spectrum sampling technique

4.3.1. Limiting fire and destroying samples when measuring Raman spectroscopy

Compared to laboratory Raman spectrometers, portable devices often have lower-quality optical sensors and are not refrigerated. Therefore, the intensity of the excitation laser is usually greater to compensate for the quality of the signal. However, high laser intensity sometimes destroys samples, especially dark samples and SERS substrates due to heat generated at laser focus or photocatalytic reaction processes.

The mini sample shift and scan device is a small XY shift table fitted with a stepper motor that moves continuously in different random steps in time and in the X, and Y directions. The laser focus point outlines a random zigzag trail in the area (3×3 mm) of the sample. This device can be easily integrated into Raman spectroscopy systems because it does not have to affect the internal structure of the instrument.

The random sample translation module on the one hand works quite effectively in limiting sample burning, on the other hand, helps to measure the average spectrum over a larger sample area, the spectrum is more representative. As shown in Figure 4.14, the black line is the Raman spectrum of the black explosive measured using the random sample shift modulus. When the sample shift module is not used, the measured spectrum is the noise line due to burnt black explosives.

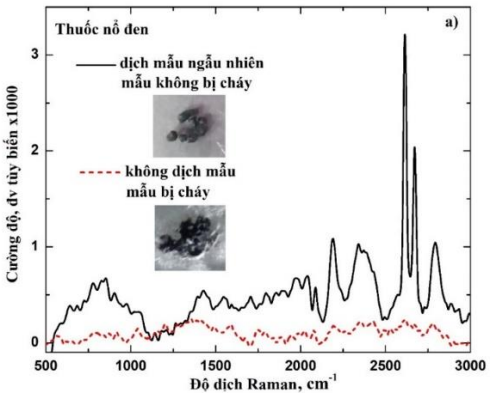

Figure 4.14. Raman spectra of black explosives were measured using a random sampler.

4.3.2. Improved SERS signal quality

The random sample translation module is also applied to sample measurement using the SERS base and demonstrates many advantages. On the one hand, this technique allows us to measure spatially averaged spectra over a relatively large area of samples. On the other hand, it helps to prevent SERS samples and substrates from laser damage. Experimental data also show that this technique allows the use of a laser beam with a power of tens of milliwatts to excite SERS samples while maintaining the same resolution.

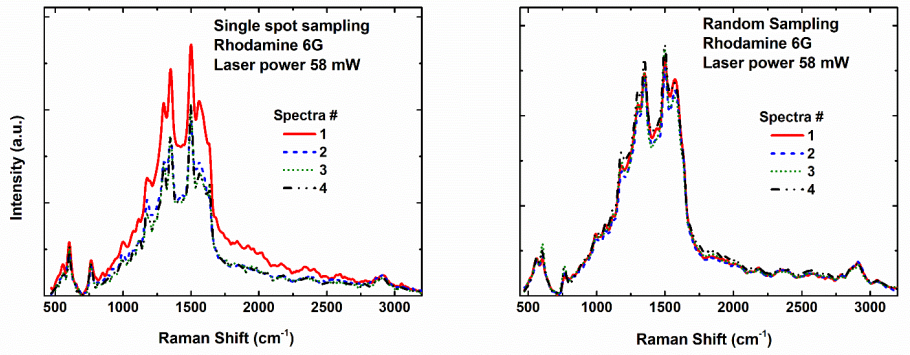

Figure 4.15. Measurement results of Rhodamine 6G Raman spectroscopy on MFON-structured SERS substrates and handheld Raman spectrometers: a) Single point measurement mode; b) Sample shaking mode. The measured source power is 58 mW.

It can be seen that, unlike the trend of decreasing spectral intensity in Figure 4.15a, the spectra in Figure 4.15b almost overlap. The movement of the table ensures that signals from new areas on the SERS substrate are collected and prevents samples from being damaged by the laser. Thus, the random sampling mode significantly improves the stability and repeatability of Raman spectra. The high stability of the signal also opens the possibility of using a random sampling technique to perform quantitative analysis using the SERS substrate using a portable Raman spectrometer.

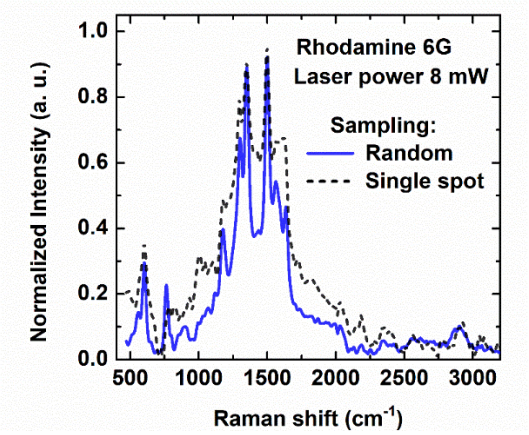

Figure 4.16. Raman spectroscopy results of Rhodamine 6G on MFON-structured SERS substrate and handheld Raman spectrometer: dashed line-single-point measurement mode; solid line-measurement mode shake sample. The laser source power is 8 mW.

Figure 4.16 shows the Raman spectrum obtained when the laser power is set to a minimum of 8 mW. The solid and dashed lines are spectra obtained in the random sample shake and single point measurement modes, respectively. It can be seen that the Raman peaks obtained by the random sample shake technique are significantly narrower than those measured in the single-point sampling mode.

Using the random sample shaking mode, the change in the Raman spectrum obtained when the laser power was adjusted from 8 to 80 mW was investigated. Figure 4.17 shows some representative Raman spectra obtained at different laser powers to demonstrate the effect.

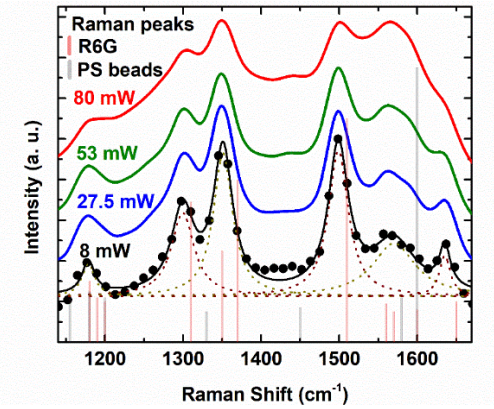

Figure 4.17. Raman spectra of Rhodamine 6G were obtained at different powers. The peak of the Raman spectrum widens with increasing laser power. The solid lines are the experimental data and the dashed lines are the vertices that are fitted using the Lorentz function. The vertical lines are the positions of the Raman peaks of Rhodamine and PS particles.

When the laser power was increased, the Rhodamine 6G spectral line was markedly widened. The intensity of the Raman peaks also increased correspondingly but at different rates. At low laser power, small peaks at 1178 and 1636 cm-1 appear clearly. However, at high laser power, these spectral peaks blend into the shoulders of larger peaks and are almost imperceptible.

CONCLUSIONS AND RECOMMENDATIONS

The thesis has achieved the following results:

1. The thesis has successfully fabricated polystyrene nanoparticles with sizes of 212 ± 3 nm, 477 ± 7 nm, 574 ± 10 nm, 684 ± 20 nm, and 812 ± 24 nm by classical condensation method. The fabricated polystyrene nanoparticles are spherical and monodisperse, these properties favor the use of polystyrene nanoparticles as masks to fabricate nanostructures.

2. The thesis has successfully fabricated monolayer films close-packed with polystyrene nanoparticles by the method of dropping and placing them on silicon and glass substrates. The fabricated particle films are monolayer and highly compact to form a hexagonal structure. This is a favorable property to fabricate highly ordered and repeatable surface Raman scattering enhanced substrates.

3. The thesis has successfully fabricated the SERS substrate with a metal film structure coated on the monolayer close-packed polystyrene nanoparticles (MFON). These SERS substrates are highly ordered, uniform, and easy to repeat. The results of optimizing Raman signal enhancement performance by particle size showed that the SERS substrate with a PS particle size of 477 nm gave the strongest enhancement performance.

4. The thesis has successfully built a Raman scattering spectrometer based on analysis and selection of components. The special feature of the device is its compact size, easy to carry and transport for field measurements. Some of the main components of the device are as follows:

- The light source uses a 638 nm laser diode, with a half-width of 0.01 nm, and a power of 120mW that can work in both pulsed and continuous modes.

- Avantes spectrophotometer (AvaSpec-UL2048L) CMOS receiver can display images, uses a flat grating of 300 lines/mm, is uncooled, sensitive in the wavelength range from 300 nm to 1100 nm.
- Sample shaking system: the thesis studies and manufactures a two-way displacement sample shaking system.

RECOMMENDATIONS

The thesis work shows the feasibility of building a complete Raman spectrometer with a compact size, easy to transport. However, there are still many aspects that need to be further researched, developed, and investigated to improve the performance of the device such as: improving the resolution, sensitivity threshold, and automatic ability of the device...

The results of fabrication and optimization of MFON-structured SERS substrates are only applicable to Rhodamine 6G reagent, further studies are needed to evaluate the ability to detect explosives in trace form using the MFON-structured SERS substrates and the Raman spectrometer that the thesis has built successfully. In addition, further studies are needed on the quantitative ability of MFON-structured SERS substrates.

NEW CONTRIBUTIONS OF THE THESIS

1. Successfully designed and built an experimental portable Raman spectrometer using a small and compact 638 nm diode laser.

2. Propose a method of random spectroscopy and make a mini sample shift module. The mini-sample shift module allows to capture of signals from a large sample area and limits sample damage when measuring. The sample translation module also helps to improve spectral quality when measured with the SERS base.

3. Developing a method to determine the PS microsphere particle size by transmission spectrum of the monolayer close-packed PS microspheres.

4. Experimental proof and simulation that suppressing the signal attenuation channel into the substrate can help improve the Raman scattering enhancement factor of the SERS substrate according to the MFON structure by more than two times.

LIST OF PUBLICATIONS

1. Tien Van Nguyen, Linh The Pham, Khuyen Xuan Bui, Lien Ha Thi Nghiem, Nghia Trong Nguyen, Duong Vu, Hoa Quang Do, Lam Dinh Vu and Hue Minh Nguyen, *Size Determination of Polystyrene Sub-Microspheres Using Transmission Spectroscopy*, Appl. Sci. 2020, 10, 5232.

2. T V Nguyen, L T Pham, B X Khuyen, D C Duong, L H T Nghiem, N T Nguyen, D Vu, D Q Hoa, V D Lam, and H M Nguyen, *Effects of metallic underlayer on SERS performance of a metal film over nanosphere metasurface*, J. Phys. D: Appl. Phys. 55 (2022) 025101.

3. Nguyen Van Tien, Nguyen Trong Nghia, Nghiem Thi Ha Lien, Vu Duong, Do Quang Hoa, Duong Chi Dung, Phan Nguyen Nhue, Nguyen Minh Hue, *Improvement of Sers Signal Measured by Portable Raman Instrument Using Random Sampling Technique*, Vietnam Journal of Science and Technology 60(2) (2022)237-244.

4. Tien Thanh Pham, Dinh Dat Pham, Thi An Hang Nguyen, Minh Thong Vu, Lien Ha Thi Nghiem, Tien Van Nguyen, Daisuke Tanaka, Duc Cuong Nguyen, *Synthesis And Optical Characterization of Asymmetric Multilayer Metal-Insulator Nanocrescent In Aqueous Solutions*, Applied Physics Express 13, 122004 (2020).

5. Nguyễn Văn Tiến, Nghiêm Thị Hà Liên, Nguyễn Trọng Nghĩa, Đỗ Quang Hòa, Vũ Dương, Nguyễn Văn Tính, Dương Chí Dũng, Nguyễn Minh Huệ, *Phát triển thử nghiệm thiết bị xách tay nhận biết chất nổ bằng phương pháp phổ tán xạ Raman*, Tạp chí Kỹ thuật và Trang bị, số 230 (11/2019), tr21-23.

6. T. V. Nguyen, L. H. T. Nghiem, N. T. Nguyen, T. Nguyen-Tran, H. M. Nguyen, *Polystyrene Sub-Microspheres: Synthesis and Fabrication of Highly Ordered Structures*, The 6th Academic Conference on Natural Science for Young Scientists, Master & Ph.D. Students from Asian Countries (CASEAN - 6), 23 - 26, Oct. 2019, Thai Nguyen, Viet Nam.

7. Nguyễn Văn Tiến, Nghiêm Thị Hà Liên, Nguyễn Trọng Nghĩa, Vũ Dương, Dương Chí Dũng, Nguyễn Minh Huệ, *Đế Sers Cấu Trúc Màng Kim Loại Phủ Trên Màng Đơn Lớp Xếp Chặt Hạt Nano Polystyren*, Hội Nghị Quang Học - Quang Phổ Toàn Quốc Lần Thứ 11 (HNQHQP-11), 04-07, Tháng 11, 2020, Hoa Binh, Viet Nam.